

PAPER • OPEN ACCESS

## Experimental study of heat and momentum exchange between a forest lake and the atmosphere in winter

To cite this article: K V Barskov *et al* 2017 *IOP Conf. Ser.: Earth Environ. Sci.* **96** 012003

View the [article online](#) for updates and enhancements.

### Related content

- [Spatio-temporal dynamics of evapotranspiration on the Tibetan Plateau from 2000 to 2010](#)  
Lulu Song, Qianlai Zhuang, Yunhe Yin et al.
- [Cumulant expansions for atmospheric flows](#)  
Farid Ait-Chaalal, Tapio Schneider, Bettina Meyer et al.
- [Turbulent momentum transport due to neoclassical flows](#)  
Jungpyo Lee, Michael Barnes, Felix I Parra et al.

# Experimental study of heat and momentum exchange between a forest lake and the atmosphere in winter

**K V Barskov<sup>1,2</sup>, R V Chernyshev<sup>2</sup>, V M Stepanenko<sup>2</sup>, I A Repina<sup>1,2</sup>, A Yu Artamonov<sup>1</sup>, S P Guseva<sup>2</sup> and A V Gavrikov<sup>3</sup>**

<sup>1</sup> A.M.Obukhov Institute of Atmospheric Physics RAS, Moscow, Russia.

<sup>2</sup> Lomonosov Moscow State University, Moscow, Russia

<sup>3</sup> P.P.Shirshov Institute of Oceanology RAS, Moscow, Russia

[Barskovkv@gmail.com](mailto:Barskovkv@gmail.com)

**Abstract.** The article presents the results of an experimental study of turbulent heat exchange between the surface of a frozen lake surrounded by forest and the atmospheric boundary layer. Heat and momentum fluxes were measured at three levels by an eddy covariance (EC) technique. Additionally, the heat fluxes were estimated by a surface energy balance method using a temperature profile measured in the snow cover and net longwave and shortwave radiation. The results of the measurements show that the eddy covariance fluxes correlate well with those obtained by the surface energy balance method, with a tendency of underestimation. The presence of wind-shear effects at treetop height demonstrated recently in a Large Eddy Simulation (LES) [3] was supported in our measurements by the fact that the momentum flux increased with height from the surface. The negative sensible heat flux increased with height most of the time. We suggest that this phenomenon may partially be caused by the high negative heat fluxes above the surface formed when warm advection occurs at altitudes of ~100 m. During the warm advection events, Monin-Obukhov similarity theory (MOST) fails to reproduce the sharp increase of the negative heat flux at the surface layer. Beyond the warm advection events, the MOST calculations agree well with the EC fluxes, however, with some systematic underestimation bias.

## 1. Introduction

Lakes cover a considerable part of Northern Eurasia and North America and make a significant contribution to heat and gas exchange between the atmosphere and the surface. To parameterize these exchanges, especially with subgrid-scale surface inhomogeneities, such as small lakes bounded by steep topography, is important for improvement of weather and climate models [1]. Lakes smaller than 10 km<sup>2</sup> account for about 54% of the global area of inland waters [2]. Many lakes in Northern Russia and Europe are surrounded by forest, and standard approaches of calculating heat exchange in the atmospheric boundary layer leads to significant errors due to the inhomogeneity of the underlying surface. In particular, landscape inhomogeneity causes changes in the statistical moments of turbulence, compared to flow over homogeneous surfaces. Thus, the application of Monin-Obukhov similarity theory (MOST) loses its theoretical grounds. Extending MOST for heterogeneous surfaces is difficult due to the lack of experimental data for the wide range of possible wind shears, stratifications, and surface discontinuity patterns.

Experimental measurement of fluxes in complex landscapes is also difficult. In particular, the results of a Large Eddy Simulation (LES) show that at distances from the forest edge less than 15-20 treetop heights the local eddy covariance (EC) momentum fluxes above the surface are caused by the velocity shear in the windstream approximately at treetop height and may differ greatly from the surface frictional stresses [3]. Such effects are inherently connected to the long-standing problem of surface energy imbalance in the EC measurements. Specifically, in most EC field experiments the energy of net



radiation minus the change of active layer heat content (ice, snow, water, or soil surface) is greater than the energy transported by turbulent fluxes of sensible and latent heat [4].

This paper presents the results of experimental studies of the turbulent structure of the atmospheric boundary layer over a small frozen lake surrounded by forest. The heat exchange of the surface with the atmosphere was estimated by various methods, specifically, eddy covariance, surface energy balance and MOST-based techniques. The experiment was conducted in wintertime over an ice-covered lake surface, to distinguish the influence of the inhomogeneous landscape on turbulence exchange in the atmosphere-surface system, and exclude the thermal effects of the lake.

## 2. Field experiment

The measurements were made in the neighborhood of a White Sea Biological Station (WSBS) operated by Moscow State University from 25.01.2017 to 03.02.2017. The measuring system was located on the lake Kislo-Sladkoe, about 2 km east of the station, near the coast of the Kandalaksha Gulf of the White Sea. The lake dimensions are approximately 200 m by 150 m. The southern and western sides of the lake are bordered by vast forest landscapes. The northern and eastern sides are bordered by a forest belt (50–100 m width) separating the lake from the gulf. There are two gaps in the forested areas about 30 m wide each that serve as open surfaces “connecting” the lake with the gulf. The terrain is hilly, while the elevations of topography around the lake do not exceed the average treetop height.

A 6-meter mast was installed in the center of the lake. The fluctuations of temperature and three wind speed components were measured using a WindMaster HS 3D Anemometer (Gill Instruments, UK) at a level of 2 m and a WindMaster 3D Anemometer (Gill Instruments, UK) at levels of 4 m and 6 m with a frequency of 20 Hz. The humidity and air temperature were measured by automatic meteorological stations Davis Vantage Pro 2 (Davis Instruments, USA) at levels of 3 m and 5 m. In addition, a gas analyzer LI-7500 (Li-Cor, USA) was installed at a level of 2 m to calculate moisture fluxes (latent heat) and carbon dioxide. The net radiation was measured using a CMP21 Pyranometer and a CGR3 Pyranometer (Kipp & Zonen, Netherlands). A soil station (Davis Instruments, USA) was mounted at a distance of about 10 m from the mast to measure the temperature of the snow cover on its surface and at the snow-ice interface (10 cm). The temperature at the bottom surface of the ice was assumed to be 0°C, with a measured ice thickness of 32 cm. Measurements on the lake were accompanied by recordings of the temperature profile in the boundary layer of the atmosphere from the surface up to 1 km with a step size of 50 m by a microwave profiler MTP-5 (Attex, Russian Federation).

## 3. Data processing

The main characteristics of the turbulent interaction of the atmospheric surface boundary layer with the surface are the sensible heat flux ( $H$ ), latent heat flux ( $L_sE$ ), and momentum flux ( $\tau$ ). These quantities represent the total fluxes where the effects of molecular exchange are negligibly small in comparison with the vertical turbulent transfer of momentum, heat, and moisture. To determine the turbulent fluxes we used an eddy covariance method, a method of surface energy balance, and a MOST-based gradient method.

### 3.1. Eddy Covariance method

The direct method, or eddy covariance method, is based on measuring the pulsations of the three wind velocity components  $u'$ ,  $v'$ , and  $w'$ , the temperature  $T'$ , and the specific humidity  $q'$  at one point above the surface. The fluxes are calculated as covariances between these variables, i.e. the second mixed moments [5]:

$$\tau = \rho_0 [\overline{u'w'^2} + \overline{v'w'^2}]^{1/2} = \rho_0 u_*^2, \quad (1)$$

$$H = c_p \rho_0 \overline{w'T'}, \quad (2)$$

$$L_sE = \rho_0 \overline{w'q'} L_s, \quad (3)$$

where  $\rho_0$  is the reference air density,  $c_p$  is the specific heat capacity of air at constant pressure,  $L_s$  is the latent heat of vaporization, and the overbar stands for the temporal average. In our case, the fluxes were

calculated by 30-minute averaging, which can be assumed to be the optimal averaging time [6]. The EC method involves special corrections to minimize errors, which are mostly of a technical nature. The corrections made to introduce the most significant changes in the heat flux are: time shifting between signals from different sensors, artificial spike removal, "plane approximation" to correct the anemometer tilt [7], Moore spectral correction [8], correction of acoustic temperature and accounting for the effect of air density fluctuations [9]. The EddyUH software package was used to compute the fluxes [10].

The sensible heat and momentum fluxes were calculated at heights of 2, 4, and 6 m with ultrasonic anemometer data at every 30-minute interval. The moisture flux was calculated at a height of 2 m.

### 3.2. Gradient method

The gradient method is based on the assumption that all statistical characteristics of the temperature, humidity, and wind velocity fields normalized to the corresponding scales of the temperature  $T_*$ , humidity  $q_*$ , and velocity  $u_*$  are described by universal functions of the dimensionless height  $\xi=z/L$ , where  $L$  is the Obukhov length and  $z$  is the level of measurements. Specifically, according to MOST the deficits of averaged meteorological variables in the surface layer obey the following relations:

$$\Delta u = u_2 - u_1 = \frac{u_*}{\kappa} \left[ \ln \frac{z_2}{z_1} - \Psi_u(\xi_2) + \Psi_u(\xi_1) \right], \quad (4)$$

$$\Delta T = T_2 - T_1 = \frac{T_*}{\kappa} \left[ \ln \frac{z_2}{z_1} - \Psi_T(\xi_2) + \Psi_T(\xi_1) \right], \quad (5)$$

$$\Delta q = q_2 - q_1 = \frac{q_*}{\kappa} \left[ \ln \frac{z_2}{z_1} - \Psi_q(\xi_2) + \Psi_q(\xi_1) \right]. \quad (6)$$

From (4) - (6) the turbulent fluxes are calculated by:

$$\tau = \rho_0 u_*^2, \quad (7)$$

$$H = -c_p \rho_0 u_* T_*, \quad (8)$$

$$L_s E = -\rho_0 L_s u_* q_*, \quad (9)$$

where  $\kappa$  is the von Karman constant, lower indices "2" and "1" denote the two levels of measurements,  $\Psi_i(\xi)$ ,  $i=u, T$ , and  $q$  are dimensionless universal functions. Thus, following MOST, one can compute the corresponding fluxes by making measurements at least on two levels.

### 3.3. Surface energy balance method

The method of surface energy balance is based on the heat conservation law: the heat entering a system equals the sum of the outgoing flux and the change of energy stored in the system. For any surface, the surface heat balance is given by:

$$R_n = H + L_s E + G, \quad (10)$$

where  $R_n$  is the net radiation at the surface, and  $G$  is the heat flux passing through the surface.

Since shortwave radiation penetrates snow and ice, the heat conduction equation in the snow and ice layers can be written as follows ("s" and "i" indices mean "snow" and "ice", respectively):

$$\rho_s C_s \frac{\partial T}{\partial t} = \frac{\partial}{\partial z} \lambda_s \frac{\partial T}{\partial z} - \frac{\partial S}{\partial z}, \quad (11)$$

$$\rho_i C_i \frac{\partial T}{\partial t} = \frac{\partial}{\partial z} \lambda_i \frac{\partial T}{\partial z} - \frac{\partial S}{\partial z}, \quad (12)$$

where  $\rho$  is the density,  $C$  is the heat capacity,  $\lambda$  is the molecular thermal conductivity,  $T$  is the temperature, and  $S$  is the flux of shortwave radiation. Then we integrate equations (11-12) over the entire thicknesses of the snow and ice, respectively, and sum up the resulting expressions. Assuming that the

molecular heat flux and the radiation flux at the ice bottom are negligible in comparison to the surface energy fluxes, we obtain the equation

$$-\lambda_s \frac{\partial T}{\partial z} \Big|_{z=0} = \rho_i C_i \frac{\partial}{\partial t} \int_{h_s}^{h_i} T dz + \rho_s C_s \frac{\partial}{\partial t} \int_0^{h_s} T dz - S \Big|_{z=0}. \quad (13)$$

In this experiment, the snow thickness during all measurements was constant,  $h_s = 10$  cm, ice  $h_i = 32$  cm, the snow temperature was measured at two points, namely, at the surface and at the boundary of snow and ice (0 and 10 cm, respectively), the temperature on the lower ice surface was taken equal to 0°C. The density of ice ( $\rho_i = 917$  kg/m<sup>3</sup>), the heat capacity of ice ( $C_i = 2150$  J/(kg K)) and snow ( $C_s = 2150$  J/(kg K)) are the tabular values, and the density of snow ( $\rho_s = 100$  kg/m<sup>3</sup>) was measured directly. The temperature integral was calculated numerically by the trapezoidal rule. The snow temperature was measured with an interval of 10 seconds.

## 4. Results

### 4.1. Comparison of heat fluxes obtained by gradient method and eddy covariance method

Stable stratification in the atmospheric surface layer was observed during the entire experiment, and all turbulent heat fluxes were directed from the atmosphere to the surface. Figure 1 shows the vertical air temperature profile up to 1 km, the sensible heat flux calculated by the gradient method, and the turbulent heat fluxes measured at heights of 2, 4, and 6 m. It can be seen that there are time intervals when the measured fluxes agreed well with the MOST calculations (gradient method), and the other cases when the MOST calculations do not fit the experimental data. Consider both scenarios in more detail:

At some time intervals (for example, those around 26.01 12:00, 31.01 00:00, 01.02 12:00) the results of the gradient method agree well with the direct measurements, albeit being smaller in absolute values. At the same time, the extrema of the heat flux observed during these periods agree well with the increase in the wind speed (up to 5-6 m/s) and with the enhanced difference in temperature between the surface and the atmosphere at the measurement level (not shown). The MOST data demonstrate these heat flux extrema as well, since the flux is proportional to the wind speed and temperature difference between the surface and the atmosphere.

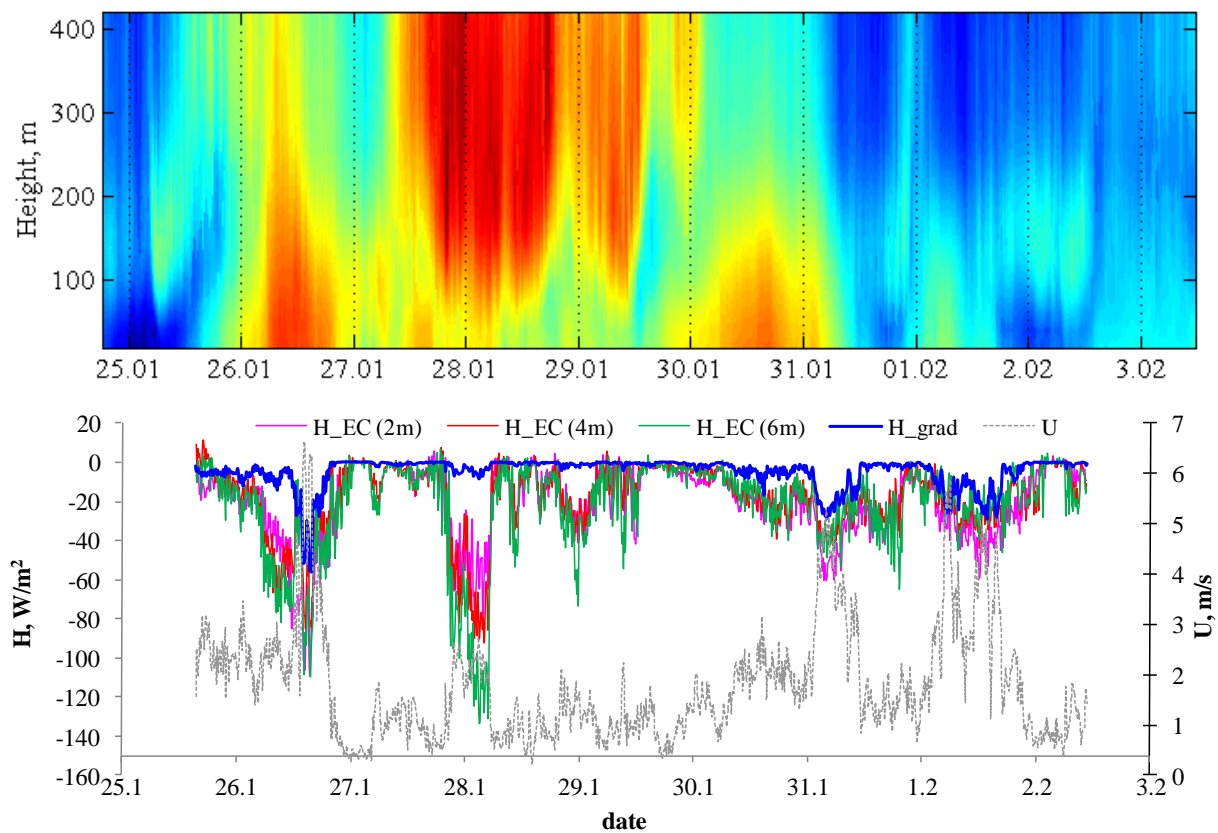


**Figure 1.** Temperature distribution in the boundary layer of the atmosphere (above) as measured by MTP-5 profiler, fluxes of sensible heat from EC measurements at different levels ( $H_{EC}$ ), sensible heat flux by the gradient method ( $H_{grad}$ ), and average wind velocity ( $U$ ).

At other time intervals (for example, those around 28.01 00:00 and 29.01 00:00) there are apparent spikes in the EC-fluxes with no corresponding extrema in the MOST-calculated fluxes. Note that in such cases the wind speed remains small ( $< 2$  m/s), so that the MOST cannot provide a significant increase in the  $H$  value. These periods coincide with warm air advection in the middle and upper part of the boundary layer (Figure 1), so that a negative heat flux may form at altitudes about 100 m, following the temperature gradient. We suggest that there may be turbulent diffusion of the heat flux from heights of about 100 m to the surface layer, where the negative heat flux is lower in absolute value. At these times we observe that the heat flux is very sensitive to the wind speed (much more than that calculated by MOST): increasing the speed from 1 m/s to 2 m/s on 28.01 causes the absolute values of fluxes to increase from  $40 \text{ W/m}^2$  to  $120 \text{ W/m}^2$ . In this case the flux significantly depends on the height; its modulus increases with height as suggested above. In particular, at 00:00 28.01 the following fluxes were observed:  $50 \text{ W/m}^2$  at a level of 2 m,  $80 \text{ W/m}^2$  at a level of 4 m, and  $120 \text{ W/m}^2$  at a level of 6 m.

A LES simulation of the atmospheric boundary layer over a lake surrounded by forest [3] demonstrated that the absolute magnitude of the heat flux resulting from the temperature differences near the surface decreases with height. In our case, by contrast, it increases with height during the large-flux events. This supports the proposed hypothesis about the role of vertical turbulent transport of heat flux.

One more striking feature seen in Figure 1 is that the measured heat fluxes significantly exceed those computed from MOST, including the periods of a weakly stratified boundary layer (1.02 – 3.02), where

the vertical heat flux diffusion is small. A feasible explanation of this is that the effect of landscape inhomogeneity leads to the development of a secondary circulation [11].

#### 4.2. Comparison of fluxes obtained by surface energy balance method and eddy covariance method

Now we consider the total heat flux  $H + L_sE$  computed from EC-measurements ( $z=2$  m) in comparison to those calculated with the surface energy balance method. Both series were smoothed to minimize noise (Fig. 2). The span for the moving average is 5.

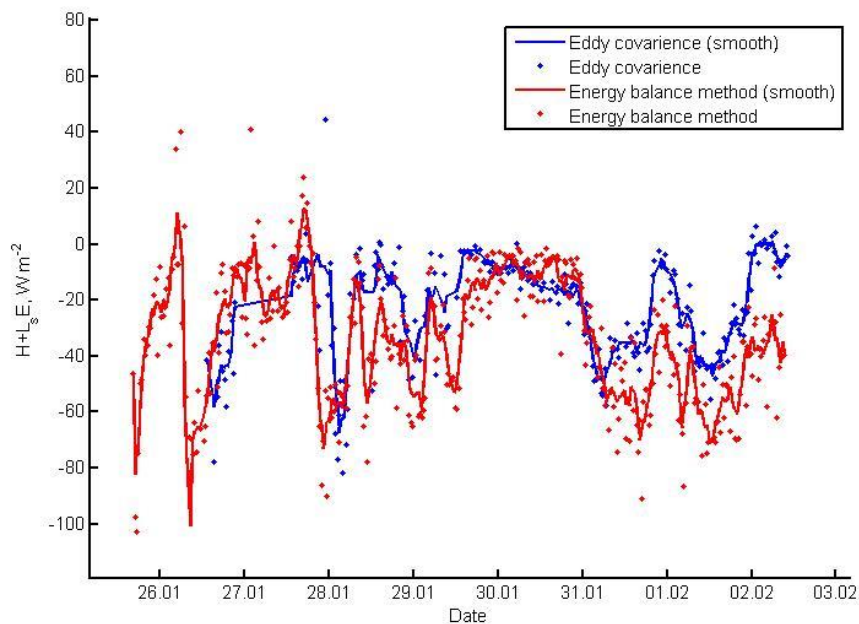


**Figure 2.** Total heat flux (sensible plus latent) according to direct measurements and calculations from surface energy balance. The span for the moving average is 5.

One can see that the time series correlate well. The greatest difference between the two methods ( $62.8 \text{ W/m}^2$ ) is observed on 28.01 during warm air advection above the surface layer. Significant discrepancies are also observed during the last two days of the experiment. In both cases the EC technique underestimates the absolute total heat flux, in line with common experience (as mentioned in the introduction). This is likely a result of the secondary circulations induced by the presence of a forest-lake boundary [11]. The mean difference between the two methods for all period is equal to  $16.8 \text{ W/m}^2$ . The correlation coefficient of the two time series is equal to 0.6.

#### 4.3. Momentum flux profile

The EC-computed momentum flux time series at each level were divided into two corresponding to different types of heat flux formation, as discussed above:

27.01 20:45 - 28.01 03:15 (MOST fails to predict heat flux).

31.01 02:15 - 31.01 07:45 (MOST predicts heat flux satisfactorily).

The profiles of the averaged momentum flux for both time intervals defined above is shown in Fig. 3.

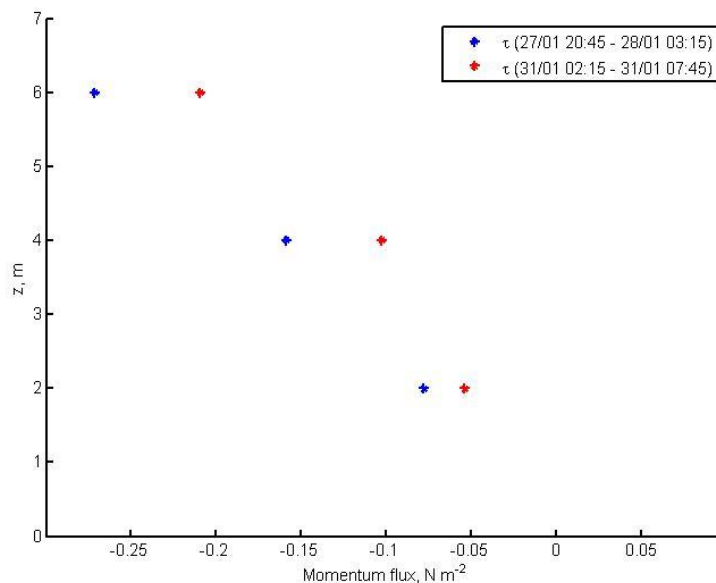


**Figure 3.** Profile of eddy covariance momentum flux.

The momentum flux increases with height as an approximately linear dependence, and at the surface the momentum flux tends to 0. This agrees well with the LES of inhomogeneous boundary layers [3]. Thus, landscape inhomogeneity is very likely to significantly impact the momentum budget in the surface layer above Kislo-Sladkoe Lake.

## 5. Conclusions

The turbulence measurements over a frozen lake surrounded by forest demonstrate that eddy covariance fluxes correlate well with those obtained by the surface energy balance method. The tendency of the EC technique to underestimate fluxes derived from the surface energy balance is in agreement with the energy balance closure problem described in [11]. This may be attributed to the secondary circulations developing near the forest-lake boundary. The presence of wind-shear effects at the height of trees demonstrated recently in LES [3] was indirectly supported in our measurements by an increase of momentum flux with height in the surface layer, extrapolating to zero at the surface. However, contrary to LES [3], the sensible heat flux decreased with height most of the time. We suggest that this may be at least partially attributable to the high magnitude negative heat fluxes above the surface layer formed when warm advection occurs at altitudes of  $\sim 100$  m. During the warm advection events MOST fails to reproduce the sharp increase of negative heat flux in the surface layer. This can be explained by the presence of a vertical transport of heat flux from above not taken into account in the theory. Beyond the warm advection events, the MOST data correspond well to the EC fluxes, however, with some systematic underestimation of the flux magnitude. This is likely to be a consequence of omitting the surface inhomogeneity effects in the MOST calculations.

## 6. Acknowledgments

This work was supported by RSF grant (17-17-01210).

**References**

- [1] Rouse W R, Oswald C J, Binyamin J, Spence C, Schertzer W M, Blanken P D, Bussieres N and Duguay C R 2005 *J. Hydromet.* **6** № 3 291–305
- [2] Downing J A, Prairie Y T, Cole J J et al. 2006 *Limnol. Oceanogr.* **51** № 5 2388–97
- [3] Glazunov A V and Stepanenko V M 2015 *Izvestia. Atmospheric and Oceanic Physics.* **51** issue 4 351-61
- [4] Foken T and Oncley S P 1995 *Bulletin of the American Meteorological Society* **76** 1191-3
- [5] Andreas E L, Jordan R E and Makshtas A P 2005 *Boundary Layer Meteorology* **114** 439–60.
- [6] Volkov Yu A and Repina I A 2002 *Surface and internal waves in the Arctic seas* ed I V Lavrenova and E G Morozov (Saint Petersburg: Gidrometeoizdat) chapter 11 pp 189-206
- [7] Wilczak J M, Oncley S P and Stage S A 2001 *Boundary Layer Meteorology* **99** 127-50
- [8] Moore C J 1986 *Boundary Layer Meteorology* **37** 17-35
- [9] Webb E K, Pearman G I and Leuning R 1980 *Quarterly Journal of the Royal Meteorological Society* **106** 85-100
- [10] [https://www.atm.helsinki.fi/Eddy\\_Covariance/EddyUHsoftware.php](https://www.atm.helsinki.fi/Eddy_Covariance/EddyUHsoftware.php)
- [11] Foken T 2008 *Ecological Applications* **18** № 6 1351-67